Ultrasound Applications in the Safety Assessment of Concrete Structures

The safety assessment of concrete structures involves regular inspections to evaluate the real condition of the structure. A concrete structure is subjected to cracking whenever the developed tensile stresses due to deterioration processes or structural loads surpass the tensile strength of the material. While some cracks may only affect aesthetics, others may impair the durability and serviceability of the concrete structure. When monitoring cracking, nondestructive techniques (NDT) are commonly used. The use of stress wave propagation methods such as ultrasound allows one to indirectly evaluate the cracking process in a convenient and fast approach. This paper discusses the application of ultrasound to assess the integrity of concrete structures subjected to cracking of different nature. In particular, plastic shrinkage cracking and the crack repair with epoxy were evaluated through ultrasound. Ultrasound energy parameters were able to indicate the extent of plastic shrinkage cracking in small mortar and concrete slabs in laboratory conditions. The ultrasonic diffusion method was evaluated for its potential use to verify the epoxy filling of surface cracks. The results obtained here expand the already wide range of applications in which ultrasound can be used to evaluate the integrity of concrete structures.

Keywords: *Ultrasound, nondestructive testing, wave parameters, crack repair, diffuse ultrasound*.

Introduction

Quality control, structural evaluation, maintenance and increasing service life have become important issues in the construction industry in recent years. The safety assessment of concrete infrastructure systems has been the subject of worldwide studies over the last few decades, since many of these structures have already reached or are close to reaching their service life.

The use of stress wave propagation methods such as ultrasound is one of the NDT methods used in the inspection of concrete structures. Ultrasound allows to indirectly estimate concrete mechanical parameters as well as to indicate the presence of internal flaws. Usually, the ultrasonic pulse velocity (UPV) is the wave parameter applied in the inspection of concrete structures (Bungey et. al. 2006). UPV has been used in the visualization of non-uniformities within the concrete member through ultrasonic tomography (Perlin and Pinto 2019), in the estimation of the depth of surface opening cracks (Pinto et. al. 2010), as well as in other applications. However, there are other lesser used wave parameters that may be more sensitive to the presence of non-homogeneities in a concrete member. Energy-based parameters and other waveform parameters have been also used to assess concrete integrity (Souza and Pinto 2020).

Recently, the diffuse ultrasound method has been applied successfully to assess small-scale damage in the concrete microstructure which cannot be detected by the common UPV method (Jiang et. al. 2019, Landis et. al. 2021). Since concrete is a heterogeneous material, when ultrasound is used at high frequency,

with wavelengths close to the size of the aggregates and/or cracks within concrete, the ultrasound wave suffers repeated reflections. As a results, multiple scattering occurs. Thus, the displacement field of the ultrasound wave losses its temporal and spatial correlation to the incident wave, becoming highly scattered. In such cases, this displacement field can be better described by the diffusion equation which yields the diffuse ultrasound parameters of diffusivity, dissipation rate and arrival time of the maximum energy (Deroo 2009). These not so common ultrasonic parameters have shown great potential in assessing concrete integrity. While the ultrasonic diffusivity is related to the microstructure, describing how quickly the ultrasonic intensity is transferred in the material, the dissipation parameter is related to linear energy loss mechanisms, characterizing the viscoelastic properties of the material.

This paper presents some results of an ongoing investigation into the wide application of ultrasound to assess the integrity of concrete structures subjected to cracking. Here, the focus is on the application of ultrasound to evaluate the extent of plastic shrinkage cracking and the crack filling process with epoxy. Previous works used ultrasound to estimate the depth of surface opening cracking (Pinto et. al. 2010), to evaluate the effectiveness of crack filling procedures (Souza and Pinto 2020), to improve ultrasound tomography (Perlin and Pinto 2019), to evaluate the stiffness loss of reinforced concrete beams due to flexure cracking (Tinoco and Pinto, 2021), among other applications.

Firstly, this work discusses the use of energy-based parameters of the ultrasonic waveform to evaluate the extent of mortar and concrete small slabs subjected to plastic shrinkage cracking. The travel path of an ultrasonic pulse suffers deviation in the presence of big non-uniformities, such as honeycombs, leading to smaller apparent pulse velocities as compared to a travel path in a sound material. However, the same effect may not be expected when small cracks are present. The variation on UPV in such cases is much smaller, being mainly dependent on the degree of cracking. Thus, the observed variations may not surpass the variations expected due to the heterogeneous nature of concrete. On the other hand, it is well recognized that cracking leads to an attenuation of the ultrasonic signal (Fernando and Suares 1987, Selleck et. al. 1998, Shiotani and Aggelis 2009) and thus, other waveform parameters may be more sensitive to a discontinuity in the travel propagation path. This research explores other stress wave parameters besides UPV, such as group velocity and energy associated parameters, and their relationship to the extent of small and randomly distributed cracks such as plastic shrinkage ones.

Secondly, the diffuse ultrasound method was used to assess the crack filling procedure with epoxy. Surface opening cracks with various depths were induced in concrete specimens. Once the crack has been fully filled, the less scattering of the ultrasound transmission should be reflected in changes on the diffuse ultrasound parameters of diffusivity, dissipation rate and arrival time of maximum energy (ATME). Thus, these diffuse parameters are associated to crack filling with epoxy. This second application follows a previous work in which the application of the ultrasound diffusion method was successfully used to monitor the development of cracking in a structural beam subjected to bending. The loss of

stiffness was directly related to changes on the diffusivity and ATME parameters (Tinoco and Pinto, 2021).

The ultrasonic parameters investigated here, both those associated to the waveform and the diffusion method were able to assess concrete integrity associated to cracking, showing that ultrasound can be a powerful tool to assess integrity of cracked concrete structures.

Ultrasound in Concrete

Ultrasonic Energy Parameters

From a typically ultrasonic waveform, such as the one shown in Figure 1, one could obtain some characteristic parameters of the waveform such as the ultrasonic pulse velocity (UPV), group velocity (V_g) and some other energy related parameters.

The UPV is the most common used parameter when ultrasound is used to evaluate a concrete structure. In order to obtain its value, there is no need to gather information about the waveform, as presented in Figure 1, but only to measure the elapsed propagation time between two transducers placed at a known distance. Portable ultrasound equipment, widely available and affordable, usually displays this value in an ultrasound reading.

Figure 1. *Typical Ultrasonic Waveform*

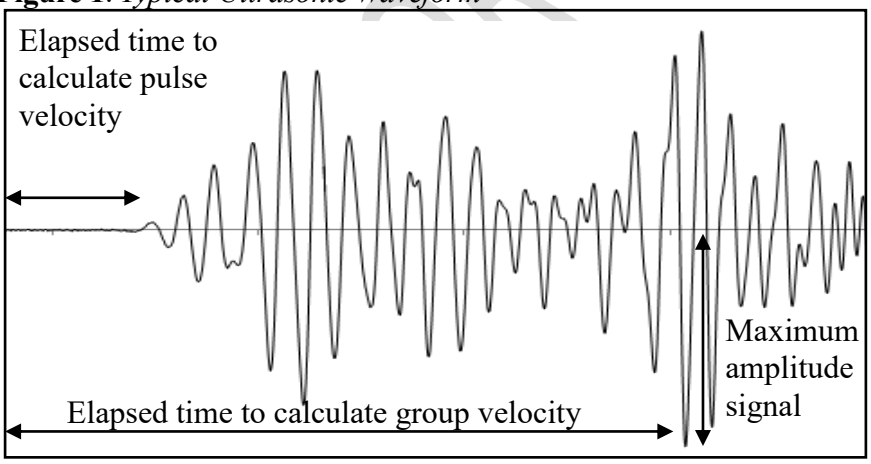

The group velocity can be considered as the velocity with which the major part of the energy propagates. When a group of waves advances in a dispersive media, the velocity of the group is less than the individual wave velocities (Graff, 1991). It can be calculated from the waveform signal by recording the time at maximum amplitude (Shiotani and Aggelis 2009).

The quantification of the energy of the ultrasonic signal can be adopted as the area under the rectified signal of the wave envelope, as given by Equation 1 (Shiotani and Aggelis 2009; Hauwert et al. 1999).

$$E = \int_0^{t_i} |A(t)| \quad dt \tag{1}$$

where:
A(t) - signal amplitude in time t;
t_i - end of time window fixed in the experiments.

The accumulated waveform energy can thus be obtained up to a certain time t_i previously fixed. This time could be the one after which there is no significant oscillation or any another threshold time before which the major part of energy has occurred.

However, the applied pressure to the ultrasound transducers has a profound effect on the waveform amplitudes, and thus on the energy value calculated by Equation 1. Therefore, energy parameters that do not rely solely on the absolute values of amplitudes recorded but rather on normalized amplitude values are desired. Aggelis and Philippidis (2004) introduced the center time parameter calculated as the time centroid of the waveform, as shown in Equation 2.

$$t_c = \frac{\int_0^{t_i} t|A(t)| \quad dt}{\int_0^{t_i} |A(t)| \quad dt} \tag{2}$$

where:
t_c - center time.

Similarly, one could calculate the time that a certain percentage of the accumulated energy has been propagated. In this study, t_{25}, t_{50} and t_{75} which correspondents to the times at which 25%, 50% and 75% of total energy have propagated were explored, according to Equation 3. Recently, Bressan at. al. (2023) used the time parameters of t_{10} and t_{25} to characterize the setting behavior of concrete.

$$x = \frac{\int_0^{t_x} |A(t)| \quad dt}{\int_0^{t_i} |A(t)| \quad dt} \tag{3}$$

where:
x - 25%, 50% or 75% in this study.

Diffuse Ultrasound Method

An ultrasonic wavefield in concrete can be regarded as the sum of a coherent ballistic field, and an incoherent diffuse field. The diffuse field occurs due to the heterogeneous nature of concrete, which causes the ultrasonic wave field to be strongly scattered. Ballistic theories give accurate results when low frequencies are used, since wavelengths are greater than the size of scatters. However, when high frequencies are used, and wavelengths are close to the size of scatters, a strong scattering regime occurs which is better modeled by the diffusion approximation (Becker et. al. 2003).

The diffusive nature can be understood as a continuous stochastic process in time. A system is described by a stochastic process when the system variables are considered random. Such randomness arises from external or internal sources, whose behavior is not completely known.The diffusion equation is a mathematical

tool that deals with these systems that are the result of many and small disturbances, each of which generates changes in the system variables in an unpredictable way (Castro 2013).

As an approximation, some assumptions are made in order to establish the energy diffusion equation for ultrasonic waves. Initially, it is assumed that the scatterers are randomly distributed. Secondly, all scattering is assumed to be elastic-linear, i.e., there is no change in the incident frequency for the reflected and the transmitted waves, with no energy lost by scattering. Further, it is assumed that the medium is isotropic, which means that the energy will travel in the same way in all directions (Deroo 2009, Arne 2014).

This dispersion process causes the energy of elastic waves to propagate in directions that do not coincide with the incident wave. Thus, the diffuse method assumes that, after successive scattering events, the spectral energy density of an ultrasonic wave field can be described by the diffusion equation. This diffuse field is spatially and temporarily incoherent with the incident signal and the variables are considered random. The diffusion theory can account for the random distribution of microcracks.

The diffusion equation in a medium is given by a second-order parabolic partial differential equation. This equation represents the spectral energy density (energy per frequency, per volume) of an ultrasonic wave field over time, as shown in Equation 4 (Weaver and Sachse, 1995; Weaver, 1998).

$$\frac{\partial\langle E(\boldsymbol{r},t,f)\rangle}{\partial t} - D\nabla^2\langle E(\boldsymbol{r},t,f)\rangle + \sigma\langle E(\boldsymbol{r},t,f)\rangle = P(\boldsymbol{r},t,f), \forall \boldsymbol{r} \in \beta \quad (4)$$

where:

$\langle E(\mathbf{r},t,f)\rangle$ - the spectral energy density per unit volume (at a time t and a frequency f), at a point in the spatial domain β specified by the vector $\mathbf{r} = r(x, y, z)$;

$P(\mathbf{r}, t, f)$ - the spectral energy density of the source;

D - diffusivity [$m^2\ s^{-1}$]

σ - dissipation rate [s^{-1}].

Both the diffusion parameters of diffusivity (D) and dissipation rate (σ) are frequency dependent. While the ultrasonic diffusivity is directly related to the concrete microstructure, describing how quickly the ultrasonic intensity is transferred in the material (Planès and Larose 2013), the dissipation rate is related to energy loss mechanisms (Weaver 1998). The dissipation rate can be related to the viscoelastic properties of the material (Anugonda et al. 2001).

From the energy curve given by Equation 4, one could obtain the arrival time of the maximum energy (ATME), another well used diffusion parameter (In et al., 2017; Quiviger et al. 2012; Seher et al., 2012).

When ultrasonic tests are performed with the intention of gathering the diffusion parameters, care should be taken regarding the distance between the transducers. This distance should be greater than the mean free path, which corresponds to the minimum distance necessary to consider the energy propagation random (Turner and Weaver 1994). The mean free path can be estimated by Equation 5 (Page et al. 1995; Weaver 1998).

$$L^* = 3D/V_e \quad (5)$$

where:

L^* - mean free path [m];

V_e - average velocity at which energy is transported [m s^{-1}]

Usually, the group velocity (V_g) is used as the velocity V_e (Page et al., 1997; Schriemer et al.,1997).

Assessment of Extent of Plastic Shrinkage Cracking with Ultrasound

Materials and Methods

Two concrete and two mortar thin slabs of 600 x 950 x 40 mm of dimensions were produced in the laboratory. The slabs were cured differently in order to induce plastic shrinkage cracking in one concrete and one mortar slab. The experimental program was based on the ones given by Kraai (1985), Ma et. al. (2004), and Pelisser et. al. (2010).

In the confection of the wooden molds, while the bottom was sealed with varnish, the sides were covered with a polyethylene film. Thus, water could only evaporate from the slab surface. Steel angles of 35 x 20 x 20 mm of size and 2.65 mm thickness were used to restrain the slab edges, and thus preventing any substantial movement. All these measures were taken to facilitate cracking. These steel angles were fixed on the bottom of the molds in pairs spaced at around 130 mm along the perimeter, as can be seen in Figure 2.

Figure 2. *Wooden molds with steel angles*

Concrete and mortar mixture proportions are presented in Table 1. A Brazilian composite cement with pozzolan addition up to 14% in mass, ASTM C

33 natural fine aggregate and coarse aggregate with maximum aggregate size of 9.5 mm were chosen.

Table 1. *Mixture proportions, in mass*

	cement	fine aggregate	coarse aggregate	w/c
concrete	1	1.26	1.96	0.51
mortar	1	1.5	-	0.47

The two concrete and the two mortar thin slabs were cast simultaneously from the same mixes. A vibrating table was used to consolidate all slabs. After casting, one concrete slab and one mortar slab were cured in the laboratory at an average temperature of 22^{o}C and average relative humidity ranging from 40% to 65%. A film of water was applied on the surface of both slabs during seven days after which the slabs were left at laboratory conditions.

The other concrete and the other mortar slabs were subjected to environmental conditions that favored plastic shrinkage cracking. Immediately after being cast, these slabs were inserted in a U-shape wooden tunnel of 500 x 700 x 500 mm of size and 1400 mm of length. At one end of the tunnel, four 250W lamps were placed in front of a 200W heater. An 80W circular fan with 400 mm diameter allowed the heated air to flow inside the tunnel. Figure 3 presents the experimental arrangement. The other end of the tunnel was covered with a plastic sheet in order to guarantee that only heated air could flow over the concrete and mortar slabs. The rate of water evaporation was measured using a small plastic container filled with concrete or mortar with dimensions of 85 x 123 x 40 mm also placed inside the tunnel. In order to ensure the occurrence of significant cracking, the mortar slab remained in the tunnel for four hours while the concrete slab for three hours after which they were left at laboratory conditions until the time of testing.

Figure 3. *Wooden Tunnel used to induce Plastic Shrinkage Cracking*

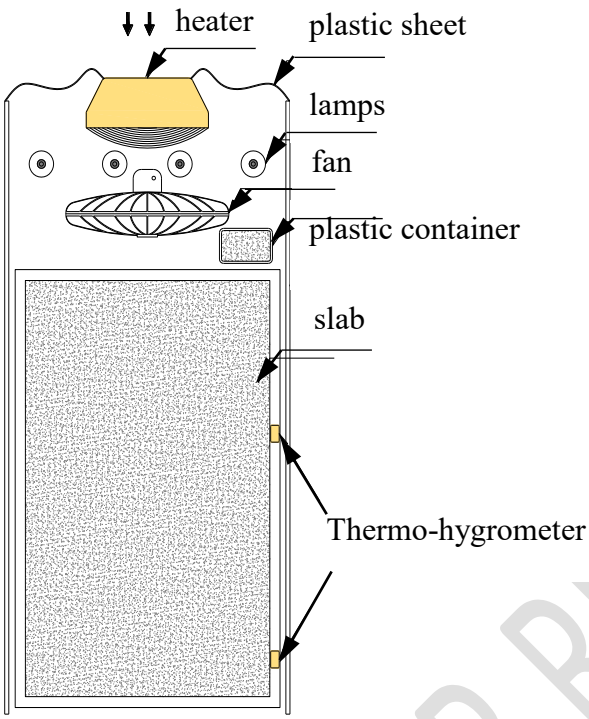

Air temperature, as well as concrete and mortar temperatures, average relative humidity were all measured with proper equipment placed inside the tunnel. The readings varied according to the distance between the equipment and the fan. Table 2 presents a summary of the readings obtained. The recorded wind speed was of the order of 4.4 km/h close to the fan, and 2.4 km/h 950 mm away from the fan.

Table 2. *Wind Speed, Temperature and Relative Humidity inside the U tunnel*

Distance from fan (mm)	Concrete		Mortar	
	temperature (°C)	relative humidity (%)	temperature (°C)	relative humidity (%)
400	50.4	25.5	48.0	25.7
800	41.8	35.6	44.9	24.0

The measured rate of water evaporation of the concrete thin slab was 1.08 kg/m^2/h whereas of the mortar thin slab was 1.91 kg/m^2/h. Figure 4 shows the obtained cracking pattern for the concrete and mortar slab, together with the identification of the principal cracks.

Figure 4. *Pattern of plastic shrinkage cracking for the concrete and mortar slabs*

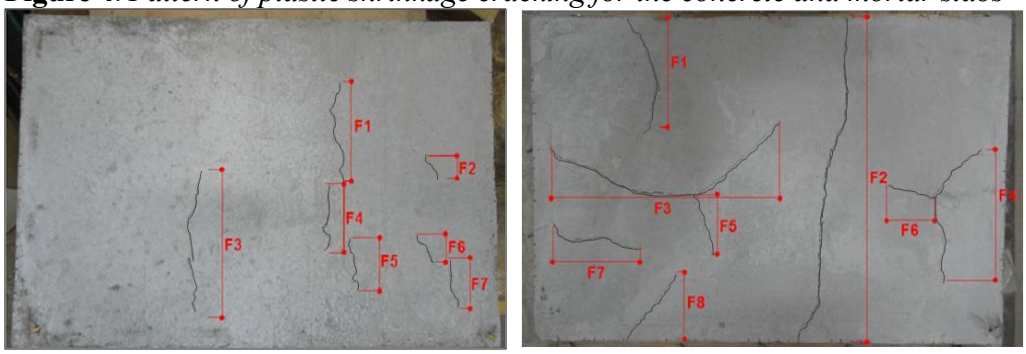

a) concrete slab b) mortar slab

In all four slabs, ultrasound tests were performed along the smallest dimension of 600 mm. Through transmission testing using the depth of the slabs was used to evaluate the whole specimen. 20 points per slab were selected. The location of each point was carefully chosen in order to prevent the steel angles to interfere with the ultrasound readings. Figure 5 shows the location of the points where ultrasonic tests were performed. Two 20 mm diameter transducers of 200 kHz were used. A layer of ultrasound gel was applied between the sensors and the specimen to ensure acoustic coupling. The input signal was a short-duration high-voltage pulse (500 V, 2.5 ms). The propagated signal was recorded at a sampling rate of 2 MHz during 1.6 ms, with a total of 3,200 data points. Around 10 readings per point were carried out. All readings were performed 30 days after the thin slabs were cast.

Figure 5. *Location of Ultrasound Reading points*

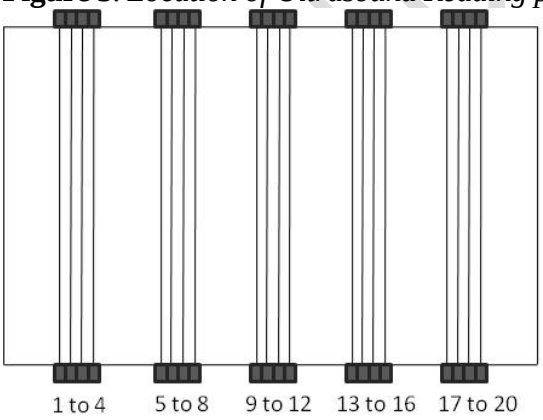

Results

Figures 6 to 9 present some of the acquired waveforms for the mortar and concrete slabs. The waveforms of Figure 6 were obtained from one of the readings on points 4 and 18 of the mortar slab not subjected to plastic shrinkage cracking, while the ones of Figure 7 came from one of the readings on the same points of the mortar slab subjected to plastic shrinkage cracking. Similarly, Figures 8 and 9 present waveforms obtained from readings on points 2 and 12 for the concrete

slabs. These readings were randomly chosen.

Figure 6. *Waveform from one reading on points 4 and 18 of the mortar slab not subjected to plastic shrinkage cracking*

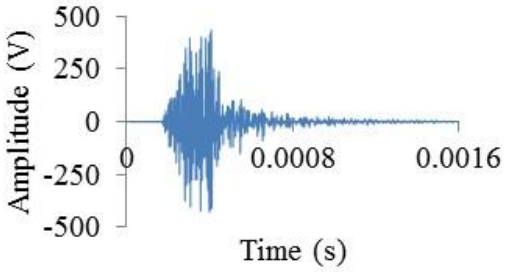

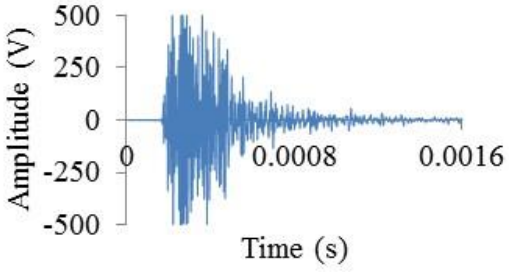

Figure 7. *Waveform from one reading on points 4 and 18 of the mortar slab subjected to plastic shrinkage cracking*

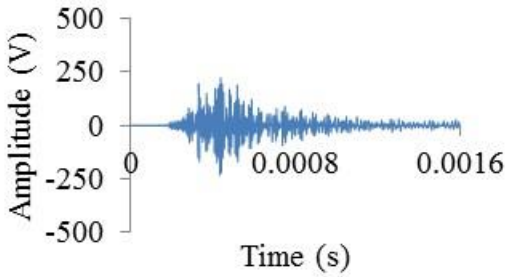

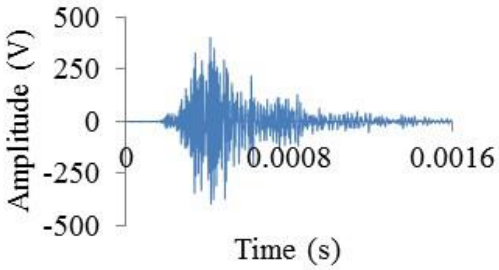

Figure 8. *Waveform from one reading on points 2 and 12 of the concrete slab not subjected to plastic shrinkage cracking*

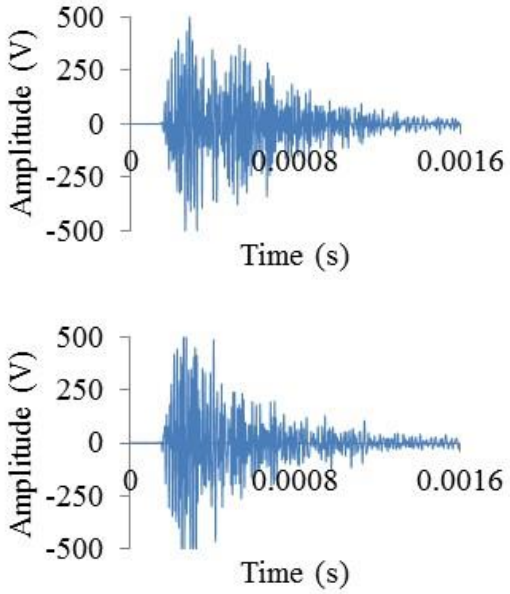

Figure 9. *Waveform from one reading on points 2 and 12 of the concrete slab subjected to plastic shrinkage cracking*

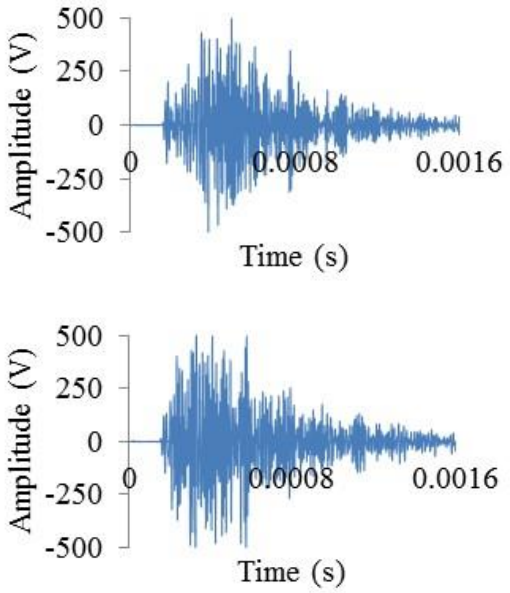

From each reading, the waveform was acquired, and the pulse velocity, the group velocity, and energy parameters given by the waveform were calculated. The energy parameters chosen were the center time, t_c, and the times correspondent to propagation of 25%, 50% and 75% of total energy, t_{25}, t_{50} and t_{75}

respectively. Equations 2 and 3 were used to calculate such parameters. The obtained values were averaged per point.

In order to describe plastic shrinkage behavior of the thin slabs, considering the randomness nature of such cracks, all waveform parameters already averaged for each of the 20 points were again averaged per slab. The obtained results are presented in Table 3, together with the coefficient of variation for each waveform parameter.

Table 3. *Final waveform parameters obtained for the thin slabs*

Waveform parameter	slab	average value	coefficient of variation
pulse velocity, m/s	sound concrete	4108	0.7%
	cracked concrete	3902	1.4%
	sound mortar	3586	1.3%
	cracked mortar	3205	16.3%
group velocity, m/s	sound concrete	2712	10.9%
	cracked concrete	1653	18.7%
	sound mortar	2849	9.1%
	cracked mortar	1638	27.4%
t_c, µs	sound concrete	574.1	2.5%
	cracked concrete	667.7	4.8%
	sound mortar	451.5	3.0%
	cracked mortar	619.3	10.2%
t_{25}, µs	sound concrete	323.5	4.7%
	cracked concrete	404.0	7.6%
	sound mortar	287.9	2.6%
	cracked mortar	388.4	12.8%
t_{50}, µs	sound concrete	489.2	4.0%
	cracked concrete	595.8	6.6%
	sound mortar	378.4	3.3%
	cracked mortar	529.5	13.1%
t_{75}, µs	sound concrete	731.1	5.7%
	cracked concrete	869.5	4.7%
	sound mortar	524.8	4.5%
	cracked mortar	784.0	11.9%

Discussion

Plastic shrinkage cracks did affect the ultrasonic waveform, as can be seen in Figures 6 to 9. There was an observed reduction on the amplitude signals for the cracked mortar and concrete slabs as compared to the slabs not subjected to cracking. This amplitude reduction was more pronounced on the waveforms obtained from the mortar slabs, especially at earlier times, thus at the beginning of the ultrasonic waveform.

Some of the waveforms in Figures 6 to 9 show signal saturation at 500V, which could affect the energy parameters given by Equations 2 and 3. However, saturation occurred only in a small range of data. Since 3,200 data points were acquired for each waveform, it was considered that signal saturation did not influence on the results.

The mean values of the waveform parameters for each of the 20 points per slab were averaged and presented in Table 3. It can be observed that the velocity parameters had their average value decreased in the slabs subjected to plastic shrinkage. On the other hand, the center time parameter and the times at which 25%, 50% and 75% of the energy has propagated increased for the cracked slabs, indicating that there was a delay on the propagation of the major part of energy.

Figures 10 and 11 present the mean values of the waveform parameters normalized to the ones obtained for the slabs not subjected to plastic shrinkage. A vertical bar representing one standard deviation variation from the mean values are also presented. It can be observed that while the average UPV value decreased only 5% for the cracked concrete slab and around 10% for the cracked mortar slab, the group velocity showed a better sensitivity, since a decrease of around 40% was observed in both concrete and mortar slabs. However, this latter parameter showed a high variability.

Figure 10. *Values of normalized waveform parameters for concrete slabs*

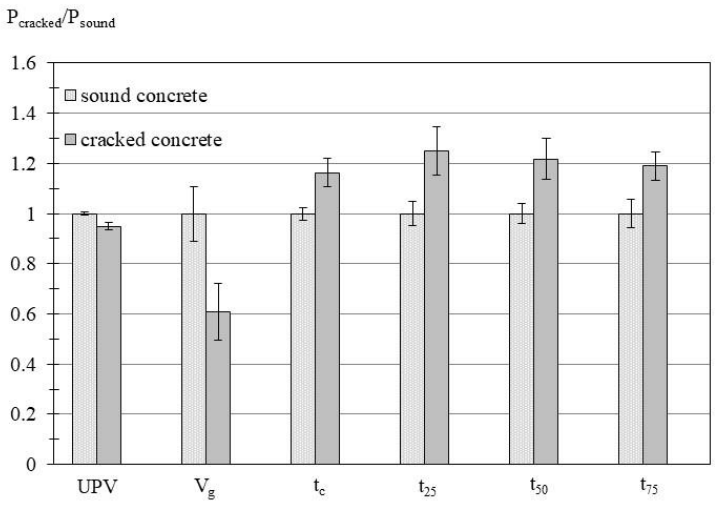

As far as the energy parameters are concerned, all four parameters (t_c, t_{25}, t_{50} and t_{75}) showed to be more sensitive to cracking than the UPV. It was observed an increase of more than 35% of their value for the mortar slab. For the concrete slab, t_{25} and t_{50} showed to be more sensitive to cracking than t_c, since their value increased more than 20%.

Figure 11 shows that due to the severe observed cracking in the mortar slabs, the obtained reduction of UPV values (around 10%) was not enough to compensate for the high variability of the data, and therefore such parameter was not able to recognize the extensive cracking suffered by the mortar slab.

Figure 11. *Values of normalized waveform parameters for mortar slabs*

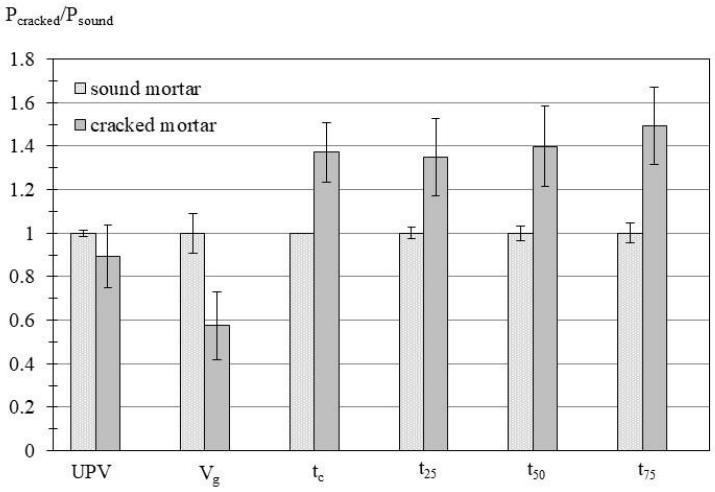

From the above discussion, it can be noticed that only relying on the UPV would not guarantee to infer plastic shrinkage cracking, even though such parameter is the most common one in ultrasound applications for concrete materials. Among the waveform parameters investigated here, the group velocity and the energy parameters were much more prone to indicate plastic shrinkage cracking.

This statement is justified by the significant lower amplitude signal values obtained at initial times associated with a delay in time of the observed maximum amplitude for the cracked slabs, as can be seen in Figures 6 to 9. The energy parameters were the ones that showed a better potential to be used to monitor cracking since their variability were lower than the one observed for the group velocity.

Evaluation of Surface Cracking Repair with Ultrasonic Diffusion Method

Materials and Methods

Three concrete prisms with artificially induced surface cracks of 3mm thickness and depths of 50 mm, 75 mm, 100 mm were cast. The cracks were latter repaired with epoxy filling. The prisms were 800 mm in length, 400 in width and 300 in height. This geometry was defined to allow the ultrasound estimation of actual crack depth according to a method previously defined (Pinto et. al. 2010).

Concrete proportions are presented in Table 4. A Brazilian composite cement with pozzolan addition up to 14% in mass, ASTM C 33 natural fine aggregate and coarse aggregate with maximum aggregate size of 19.0 mm were chosen. The compressive strength at 28 days reached 20 MPa.

Table 4. *Mixture proportions, in mass*

cement	fine aggregate	coarse aggregate	w/c
1	2.16	2.43	0.53

The cracks were artificially produced according to the following procedure. A 3mm plate was placed on the side of the specimen during casting; after approximately six hours, the plate was removed, and the artificial crack was thus formed. The ultrasound measurements were performed on the side of the specimen, after being rotated 90^{o}, allowing a flat and smooth surface and the same level of consolidation. Further details of the experimental methods can be found at Souza and Pinto, 2020.

After 28 days of casting, longitudinal wave transducers of 200 kHz with 20 mm diameter were placed 100 mm equidistant from the induced crack in the center of the sample, leading to a distance between transducers of 200 mm. Fourteen ultrasonic measurements were performed with the indirect mode of transmission, and a sampling frequency of 2 MHz. Next, the cracks were then completely filled with epoxy. After a curing period of 21 days, new ultrasound measurements were performed following the same procedure as before.

The chosen 200 kHz transducer frequency and 200 mm distance between transducers were suitable to the application of the diffusion ultrasound method. Considering a UPV of around 4000 m/s, the resultant 20 mm wavelength is of the order of the coarse aggregate. Also, considering common values of group velocity of 2500 m/s, and diffusivity of 25 m^2s^{-1}, the resultant mean free path of around 3 cm is smaller than the transducers distance.

A MATLAB code was implemented to process the ultrasonic signals obtained experimentally. The procedure for obtaining the experimental spectral energy density from a signal measured in the time domain was performed through a time-frequency analysis, associated with a fit between the experimental energy density curves and the analytical solution. The procedure is fully descried at Tinoco and Pinto, 2021. Following this procedure, the diffusion parameters of diffusivity (D), dissipation (σ) and ATME were gathered from each waveform.

Results

Figure 12 shows the approximation of the spectral energy density for a sample with the 100 mm crack. Similar curves were found for the other specimens. The diffuse parameters of diffusivity, dissipation rate and ATME were recovered from the best fit curve through the Matlab code developed. These parameters are presented in Table 5 for all specimens before and after the crack filling repair with epoxy.

Figure 12. *Spectral energy density curves for 100-mm crack specimen*

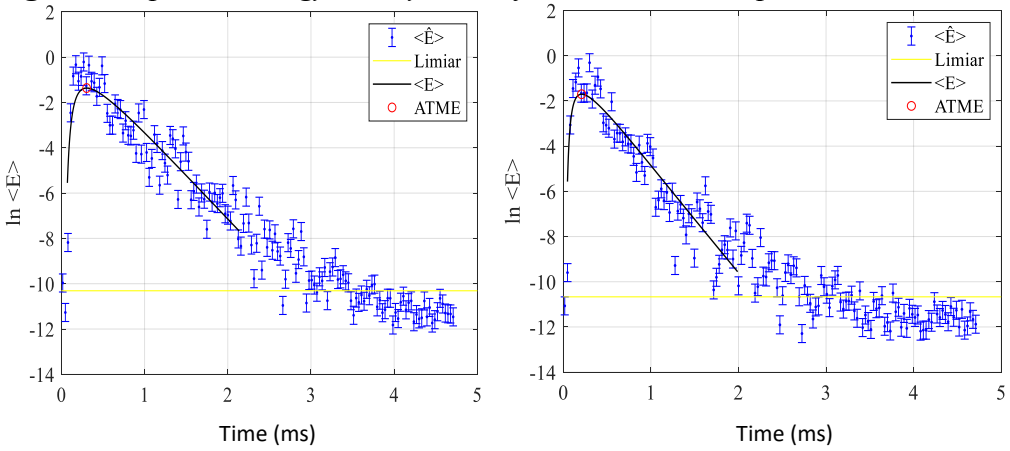

a) empty crack b) crack filled with epoxy

Table 5. *Diffusion parameters according to crack filling*

Crack depth (mm)	Diffusivity (m^2/s)		Dissipation rate (ms^{-1})		ATME (μs)	
	before	after	before	after	before	after
50	17.05	22.62	5.35	5.78	243.0	201.5
75	13.00	26.68	6.55	5.16	264.5	191.0
100	15.13	24.78	3.80	4.69	303.0	208.5

Figure 13 shows the ultrasonic signal that generated the experimental data related to the spectral energy density shown in Figure 12, and the spectral energy density curve obtained from the parameters D, σ retrieved from the approximation. Both curves were normalized for a better visualization of the energy density envelope.

Figure 13. *Normalized energy density envelope for 100-mm crack specimen*

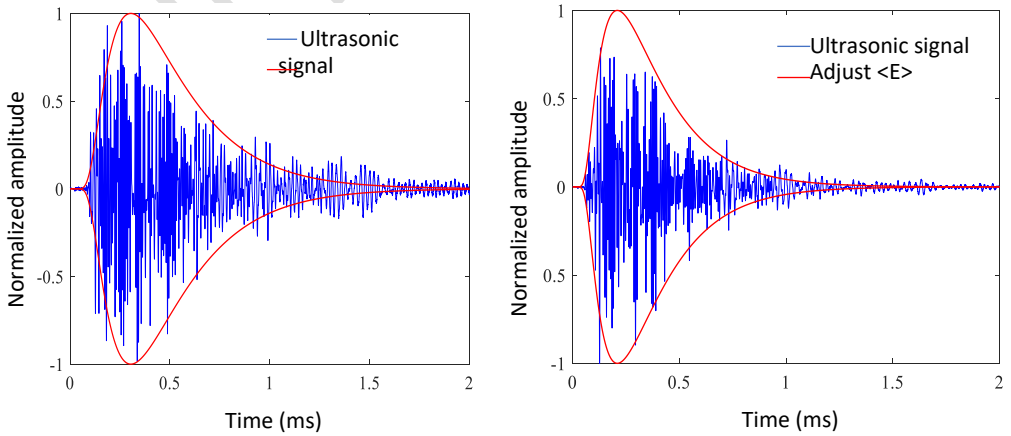

a) empty crack b) crack filled with epoxy

Discussion

Table 5 shows that the diffusion parameters of diffusivity and ATME were sensitive to crack filling. For all sizes of crack evaluated, while diffusivity increased when the crack was filled with epoxy, ATME decreased. There was not an observe trend on the dissipation rate values.

Once the crack was filled, the ultrasound signal suffered less scattering. Less scattering led to an ultrasonic faster transmission which caused the higher observed diffusivity values. Since diffusivity is directly related to the ease of ultrasonic transmission within a sample, higher diffusivity values were expected for the samples with crack filled with epoxy.

The dissipation parameter is related to the viscoelastic properties of the material, which was not significantly affected by the process of filling the cracks with epoxy for any of the crack depth studied here.

Since the ultrasound transmission was facilitated once the crack was filled, the arrival time of the maximum energy shifted to earlier times leading to smaller ATME values.

Figure 14 presents the mean values of the diffusion parameters obtained after the crack filling process normalized to the ones obtained when the crack was empty. A vertical bar representing one standard deviation variation from the mean values are also presented. It can be observed that the diffusivity value increased at least 33% for the depth cracks studied here, with no trend of increasing value with increasing of depth crack. On the other hand, the ATME parameter decreased more as crack depth increased, with a decreased on the order of 30% for the higher crack depth of 100 mm. No significant variation was observed for any of the diffusivity parameters gathered.

Figure 14. *Values of normalized diffusion parameters*

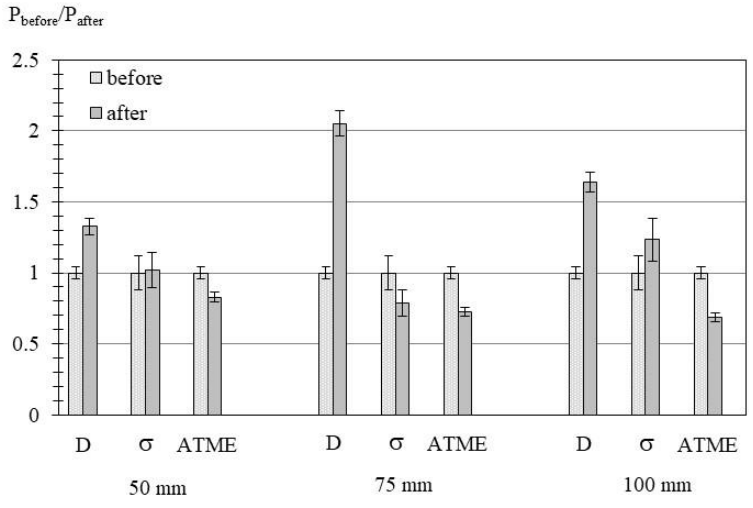

Conclusion

This study presented the importance of nondestructive methods based on stress waves to indicate the influence of cracks when assessing a concrete structure.

Ultrasound was able to detect the occurrence and the degree of cracking in concrete as well as in mortar structures subjected to plastic shrinkage cracking. Although it is common to use only the ultrasonic pulse velocity in ultrasound application, this study showed that other parameters based on the waveform such as group velocity and energy-based parameters may be useful to better indicate the extension of cracking or to continuously monitor the development of cracking.

For the slabs subjected to plastic shrinkage cracking investigated here, ultrasound pulse velocity was the waveform parameter that suffered the least variation as compared to other waveform parameters. This observation indicates that in order to evaluate the degree of cracking in a concrete structure, UPV is not the waveform parameter to be used, differently from other applications. The energy related parameters showed to be the best indicators due to the significant change in their mean values associated to a smaller variability as compared to group velocity. Even though surface cracks are easy to monitor by observation, this research showed that the use of energy parameters from the ultrasonic waveform has a potential to better indicate the degree of cracking.

As far as assessing crack filling with epoxy, this research showed that the use of diffusion parameters indicates if the crack has been treated and thus filled with the epoxy material, here utilized. The diffusivity and the ATME parameters suffer significant variation after the crack was filled. Since ultrasound transmission is facilitated once the crack was filled, the diffusivity parameter increased while the arrival time at maximum energy (ATME) decreased. This trend was observed for surface opening cracks of 3-mm widths and depths varying from 50 to 100 mm. The dissipation rate parameter did not show to be able to indicate crack filling.

These two applications here investigated together with the previous works performed by the research group expand the already wide range of applications in which ultrasound can be used to evaluate the integrity of concrete structures.

References

Aggelis DG, Philippidis TP (2004) Ultrasonic wave dispersion and attenuation in fresh mortar. *NDT&E International* 37:617-631.

Arne KC (2014) *Crack depth measurement in reinforced concrete using ultrasonic techniques.* Master's thesis, School of Civil and Environmental Engineering, Georgia Institute of Technology.

Anugonda P, Wiehn JS, Turner JA (2001) Diffusion of ultrasound in concrete. *Ultrasonics* 39:429–435.

Becker J, Jacobs LJ, Qu J (2003) Characterization of cement-based materials using diffuse ultrasound. *Journal of Engineering Mechanics* 129(12):1478–1484.

Bressan HFG, Carraro F, Pinto RCA (2023) Ultrasound monitoring of setting behavior of concrete mixtures. *IBRACON structures and Materials Journal* 16 (6).

Bungey JH, Millard SG, Grantham MG (2006) *Testing of Concrete in Structures*. 4. ed. New York: Taylor & Francis.

Castro M T (2013) *Processos estocásticos e equação de difusão: uma abordagem via o formalismo de Paul Lévy para funções características.* Ph.D. Thesis, University of Brasilia.

Deroo F (2009) *Damage detection in concrete using diffuse ultrasound measurements and an effective medium theory for wave propagation in multi-phase materials*. M. Sc. Thesis Georgia Institute of Technology, Atlanta.

Fernando V, Suaris W (1987), Detection of crack growth in concrete from ultrasonic intensity measurements. *Materials and Structures* 20:214-220.

Graff KF (1991) *Wave Motion in Elastic Solids*. New York:Dover Publication.

Hauwert AV, Delannay F, Thimus JF (1999) Cracking behavior of steel fiber reinforced concrete revealed by means of acoustic emission and ultrasonic wave propagation. *ACI Materials Journal* 96(3):291–296.

In C.-W, Arne K, Kim J.-Y., Kurtis KE, Jacobs LJ (2017) Estimation of crack depth in concrete using diffuse ultrasound: validation in cracked concrete beams. *Journal of Nondestructive Evaluation* 36(4):1–9.

Jinag H, Zhan H, Zhang J, Jiang R (2019) Diffusion Coefficient Estimation and Its Application in Interior Change Evaluation of Full-Size Reinforced Concrete Structures. *Journal of Materials in Civil Engineering*. 31(3): 1-10.

Kraai PP (1985) A proposed test to determine the cracking potential due to drying shrinkage of concrete. *Concrete Construction*. 775–778.

Landis EN, Hassefras E, Oesch TS, Niederleithinger E (2021)Relating ultrasonic signals to concrete microstructure using X-ray computed tomography. *Construction and Building Materials*. 268:12-124.

Ma Y, Zhu B, Tan M, Wu K (2004) Effect of Y type polypropylene fiber on plastic shrinkage cracking of cement mortar. *Materials and Structures* 37:92-95.

Page JH, Schriemer HP, Bailey AE, Weitz DA (1995) Experimental test of the diffusion approximation for multiply scattered sound. *Physical Review E* 52(3): 3106–3114.

Page JH, Schriemer HP, Jones IP, Sheng P, Weitz DA (1997) Classical wave propagation in strongly scattering media. *Physica A: Statistical Mechanics and its Applications* 241(1-2):64-71.

Pelisser F, Santos Neto AB, Rovere HL, Pinto RCA (2010) Effect of the addition of synthetic fibers to concrete thin slabs on plastic shrinkage cracking. *Construction and Building Materials* 24:2171–2176.

Perlin LP, Pinto RCA (2019) Use of network theory to improve the ultrasonic tomography in concrete. *Ultrasonics* 96:185-196.

Pinto RCA, Medeiros A, Padaratz I J, Andrade PB (2010) Use of Ultrasound to Estimate Depth of Surface Opening Cracks in Concrete Structures. *E-Journal of Nondestructive Testing and Ultrasonics* Oct:1-11.

Planès, T, Larose E (2013) A review of ultrasonic Coda Wave Interferometry in concrete. *Cement and Concrete Research* 53:248-255.

Quiviger A, Payan C; Chaix J-F, Garnier V, Salin J (2012) Effect of the presence and size of a real macro-crack on diffuse ultrasound in concrete. *NDT&E International* 45(1): 128-132.

Schriemer HP, Cowan ML, Page JH, Sheng P, Liu Z, Weitz DA (1997) Energy velocity of diffusing waves in strongly scattering media. *Physical Review Letters* 79(17): 3166.

Seher M, In C-W, Kim J-Y, Kurtis KE, Jacobs LJ (2012) Numerical and Experimental Study of Crack Depth Measurement in Concrete Using Diffuse Ultrasound. *Journal of Nondestructive Evaluation* 32(1): 81-92.

Selleck S F, Landis E N, Peterson M L, Shah S P, Achenbach J D (1998) Ultrasonic

investigation of concrete with distributed damage. *ACI Materials Journal* 95(1):27-36.

Shiotani T, Aggelis DG (2009) Wave propagation in cementitious material containing artificial distributed damage. *Materials and Structures* 42:377-384.

Souza FC, Pinto RCA (2020) Ultrasonic investigation on the effectiveness of crack repair in concrete. *IBRACON structures and Materials Journal* 13 (5).

Tinoco IV, Pinto RCA (2021) Evaluation of stiffness loss of reinforced concrete beams using the diffuse ultrasound method. *Ultrasonics* 117, 106540.

Turner JA, Weaver RL (1994) Radiative transfer of ultrasound. *The Journal of the Acoustical Society of America* 96(6): 3654-3674.

Weaver RL, Sachse W (1995) Diffusion of ultrasound in a glass bead slurry. *The Journal of The Acoustical Society of America* 97(4): 2094-2102.

Weaver R (1998) Ultrasonics in an aluminum foam. *Ultrasonics* 36(1-5): 435-442.